

Theme 02-1-1086-2009/2023

## Strangeness in nucleon and nuclei

### The HyperNIS project

Report on 2019-2021 upgrade of the spectrometer

*V.D.Aksinenko, A.V.Averyanov, A.E.Baskakov, S.N.Bazylev, V.F.Chumakov,  
D.V.Dementiyev, A.A.Fechtchenko, A.A.Fedyunin, I.A.Filippov, S.V.Gertsenberger,  
A.M.Korotkova, D.O.Krivenkov, R.I.Kukushkina, J.Lukstins, A.I.Maksimchuk,  
O.V.Okhrimenko, A.N.Parfenov, N.G. Parfenova, S.N.Plyashkevich, P.A.Rukoyatkin,  
R.A.Salmin, A.Sheremetiev, A.V.Shipunov, M.Shitenkov, A.V.Shutov, I.V.Slepnev,  
V.M.Slepnev, E.A.Strokovsky, A.L.Voronin*

(VBLHEP JINR)

*S.V.Tereschenko, V.V.Tereschenko*

(DLNP JINR)

*S. Pospisil, J.Smejkal, V. Sopko, P. Manek*

Institute of Experimental and Applied Physics (IEAP), Czech Technical University  
Prague, Czech Republic

*P.I.Kharlamov, M.G.Korolev, M.M.Merkin*

SINP Lomonosov Moscow State University,

*T.Nakano, M.Yosoi*

RCNP, Osaka University Japan

Project leaders E.A.Strokovsky, J.Lukstins

#### Abstract

The experimental program of the HyperNIS project is aimed at the investigation of the role which strangeness plays in nuclei (open strangeness in hypernuclei) and in nucleon (correlated  $\bar{s}s$  pair, i.e. hidden intrinsic strangeness). Initially the program consisted, respectively, of two parts to be realized with the HyperNIS spectrometer. Taking into account the spectrometer capacity, our efforts are concentrated on hypernuclear research.

The first part of the program is aimed at studying the lightest neutron-rich hypernuclei; in particular, it is necessary to establish firmly if the hypernucleus  ${}^6_{\Lambda}\text{H}$  really exists. It should be noted that in the same experiment the lifetimes and production cross sections of  ${}^4_{\Lambda}\text{H}$  and  ${}^3_{\Lambda}\text{H}$  will be investigated. If the existence of  ${}^6_{\Lambda}\text{H}$  is confirmed it will be naturally to push forward the investigation of  ${}^6_{\Lambda}\text{H}$  properties and the search for  ${}^8_{\Lambda}\text{H}$ , the most neutral nucleus among relatively heavy and complicated nuclei. The further experiment will be the study of  ${}^6_{\Lambda}\text{He}$ , previously observed only in emulsion experiments. The next step of this program is aimed to determine the binding energy of the loosely bound  ${}^3_{\Lambda}\text{H}$  hypernucleus.

The spectrometer has been upgraded: new readout electronics have been elaborated and installed, as well as new power supply modules for proportional chambers. The RPC wall has been installed for TOF measurements (slow pions),

all modules of VME crate (TQDC, synchronization) are new, as well as server, trigger modules, high voltage and gas supply systems. The spectrometer is ready for the first hypernuclear experiments. Meanwhile, the spectrometer site can be adapted for the apparatus of Short Range Correlations experiment as well, and this possibility will be analyzed to present a new project for two experiments.

## 1 Introduction

The project is aimed to study the lightest neutron-rich hypernuclei; in particular, to search for (study of)  ${}^6_{\Lambda}\text{H}$ . Simultaneously, the lifetimes and production cross sections of  ${}^4_{\Lambda}\text{H}$  and  ${}^3_{\Lambda}\text{H}$  will be studied in the same experiment because we will use the reaction  ${}^7\text{Li} + \text{C} \rightarrow {}^A_{\Lambda}\text{H} + \text{K} + \text{p(d,t,n)} + \dots \rightarrow {}^A\text{He} + \pi^- + \dots$  (where  $A=3,4,6$ ). Moreover, the production of  ${}^4_{\Lambda}\text{H}$  and  ${}^3_{\Lambda}\text{H}$  hypernuclei is the precise reference signal to ensure that  ${}^6_{\Lambda}\text{H}$  should be seen or that there are no stable forms of  ${}^6_{\Lambda}\text{H}$  if it is not observed in the same run. This task is regarded as the very first experiment because in the Frascati experiment [1, 2, 3] the evidence of only three events was reported and controversial data were obtained at J-PARC [4], where no signal was detected (instead of the expected 50 events). On the other hand, before the J-PARC experiment, A.Gal predicted that the possibility to see the  ${}^6_{\Lambda}\text{H}$  signal was low in this case because the spectrometer at J-PARC is not well suited to the task – the energy of the recoil nuclei is too high, while the pion beam produces hypernuclei of high excitation levels, that may be impossible in case of low hypernucleus binding energy. Moreover, to produce  ${}^6_{\Lambda}\text{H}$  using  ${}^6\text{Li}$  target, a double charge exchange reaction is necessary. The process is suppressed, and a lot of uncertainties should be solved to predict production rate.

The result of the  ${}^6_{\Lambda}\text{H}$  hypernucleus search should be a turning point of our program. If the  ${}^6_{\Lambda}\text{H}$  production cross section is high enough and the event yield is large, one should choose between two ways – either to continue the study of  ${}^6_{\Lambda}\text{H}$  properties or to search for  ${}^8_{\Lambda}\text{H}$  hypernucleus. It seems that the search for and possible discovery of the  ${}^8_{\Lambda}\text{H}$  hypernucleus will be the best decision. Moreover, it is a very difficult task to investigate  ${}^8_{\Lambda}\text{H}$  using pion or kaon beams. The results of these two experiments will determine if it is useful to study the properties of the new hypernuclei or to turn to the  ${}^6_{\Lambda}\text{He}$  and  ${}^3_{\Lambda}\text{H}$  hypernucleus program.

The study of poorly investigated hypernucleus  ${}^6_{\Lambda}\text{He}$  will be a natural continuation of Li beam experiments. With carbon beams, the program can be extended by determining  $\text{AN} \rightarrow \text{NN}$  weak interaction effective Hamiltonian.

An original and attractive idea is the experimental estimation of the binding energy of the loosely bound  ${}^3_{\Lambda}\text{H}$  hypernucleus. Here the approach suggested in the Laboratory of High Energies (JINR, Dubna) will be used. In this approach, the hypernuclei under study are produced by the excitation of the beam nuclei from the hypernuclei decay is being observed at a distance of tens of centimeters from the production target. Thus, the passage of the hypernuclei “beam” through materials with different  $Z$  can be investigated in order to obtain experimental estimation of the  ${}^3_{\Lambda}\text{H}$  binding energy.

## 2 Physics motivation

The Hypernuclear program in Dubna [5, 6] was started in 1988 with the setup based on a 2-m streamer chamber. The investigation of the light hypernuclei production and decay [7] was carried out, namely, the lifetime of  ${}^4_{\Lambda}\text{H}$  and  ${}^3_{\Lambda}\text{H}$ , as well as their production cross sections, were measured. It has been shown that the approach, in which the momentum of hypernuclei produced in the beams of relativistic ions is close to the momentum of the projectiles, was quite effective for measuring of hypernuclei lifetimes and production cross sections. The dedicated and very selective trigger on two body hypernuclei decays with a negative pion was the key point of this approach. Therefore, the accuracy of lifetime measurements was restricted only by statistical errors. The values of the experimental cross section were in good agreement with the results of the calculations (refs. [8] of H.Bandō, M.Sano, J.Žofka and M.Wakai, see also review [9]) performed using the coalescence model. It should be noted that hypernucleus lifetime up to now remains an actual problem. At the Conference HYP2015 on hypernuclear physics (Sendai, Japan, 2015), a special section was organized to discuss the puzzle of the light hypernuclei low lifetime. Most of the measurements [10, 11, 12] have shown  ${}^3_{\Lambda}\text{H}$  lifetime values of 140-200 ps (155ps at STAR, 181ps at ALICE), while the theory predicts 240-260 ps (256 ps, H.Kamada [13], 233-244 ps, T.Motoba [14]). For example, see Fig. 1. At the next Conference controversial  ${}^3_{\Lambda}\text{H}$  lifetime results were reported by ALICE  $\tau = 223^{+41}_{-33}(\text{stat.}) \pm 20(\text{syst.})\text{ps}$  [15] and STAR  $\tau = 142^{+24}_{-21}(\text{stat.}) \pm 29(\text{syst.})\text{ps}$  [16]. See Fig. 2.

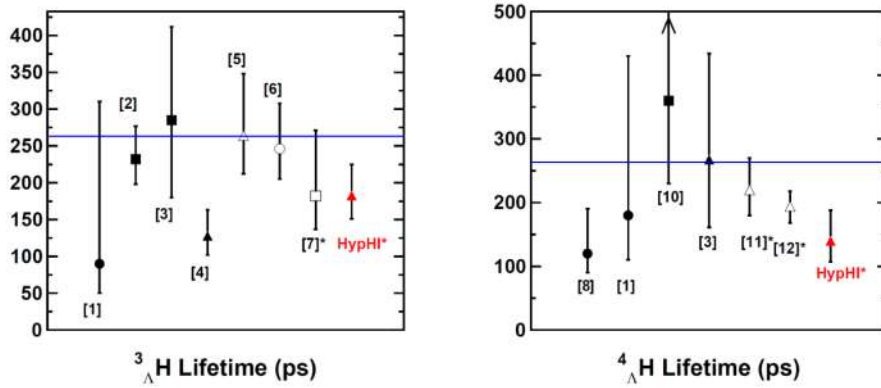


Figure 1: World data comparison of  ${}^3_{\Lambda}\text{H}$  and  ${}^4_{\Lambda}\text{H}$  lifetimes presented by Rappold in Proceedings [12] where references are listed. It should be said that the  ${}^4_{\Lambda}\text{H}$  lifetime value noted as [11] is the result of our previous experiment [17]. The values deduced in the HypHI experiment are indicated by "HypHI". The horizontal line at 263.2 ps shows the known lifetime of the  $\Lambda$  hyperon. References to counter experiments are marked by an asterisk.

In all previous hypernuclei experiments (except the above mentioned Dubna experiments and the Heavy Ion Beam experiment at GSI, Darmstadt [18, 19]) the hypernuclei are produced in various processes of target excitation. A common feature of all such experiments is the momenta of the produced hypernuclei are low and they decay almost at the production point inside the target. On the contrary, in Dubna experiments [20], the energy of hypernuclei is only slightly lower than that of the beam nuclei (see Fig. 3).

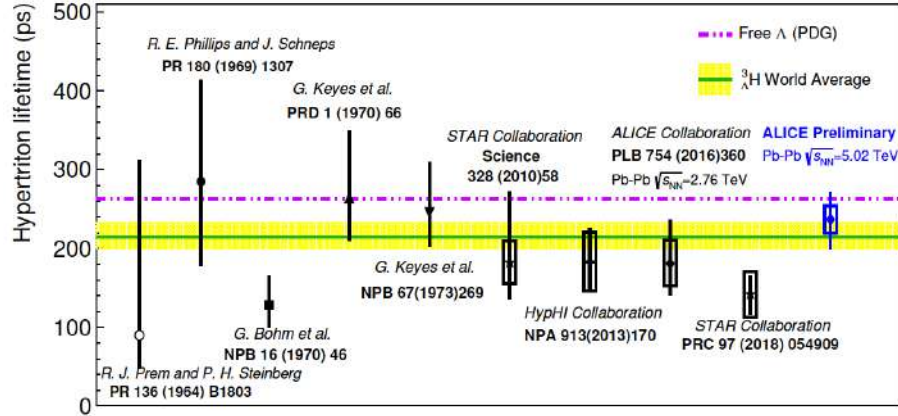


Figure 2: It can be seen that 3 years later STAR result is low, while the ALICE measurement gives much higher value. Presented by ALICE team at HYP2018 Conference [15].

Therefore, the hypernuclei lifetime in the laboratory reference frame is increased by the Lorentz factor 3-7, and a significant part of the hypernuclei decays far behind the production target. Thus, the location of the decay vertices can be used for identification of the hypernuclei decay and for determination of the lifetime of the observed hypernuclei by measuring of their flight path distribution.

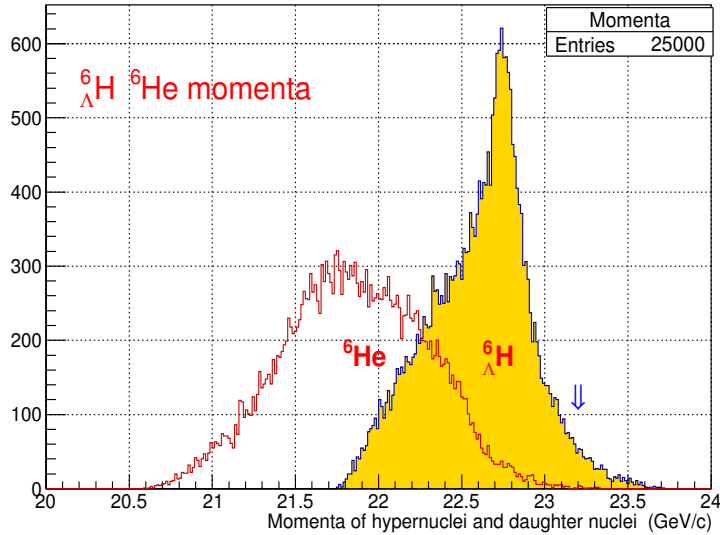


Figure 3: Expected distribution of  ${}^6_{\Lambda}\text{H}$  hypernuclei and daughter He momenta. The arrow shows the beam momentum (23.2 GeV/c). Due to Fermi motion and beam fragmentation, momenta of few hypernuclei is higher than the mean momentum value for 6 nucleons ( ${}^7\text{Li}$  beam).

The HyperNIS program is focused on **the properties of neutron rich halo hypernuclei**. In the last time, the properties of neutron rich hypernuclei and double hypernuclei are highly anticipated to revise the theory (EOS) of neutron stars to solve

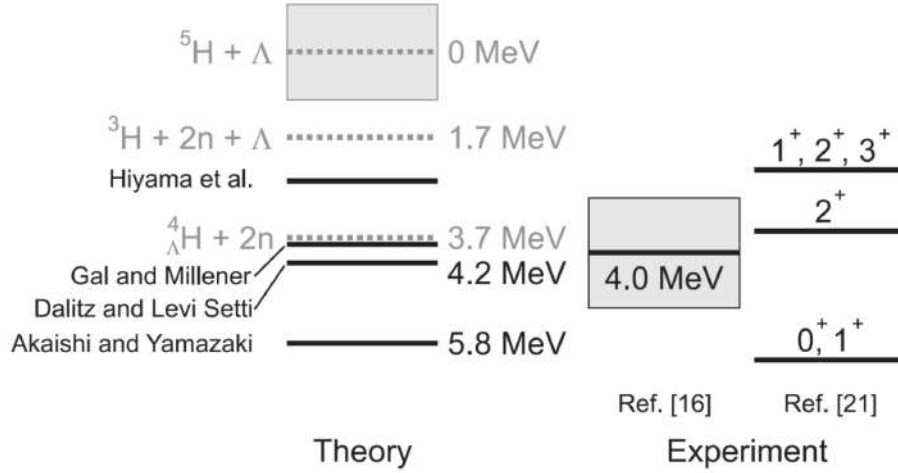
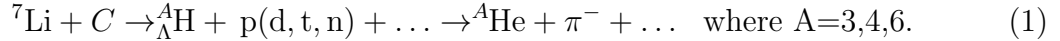


Figure 4: A summary of energy levels of  ${}^6_{\Lambda}\text{H}$ . The right side shows the energy levels and binding energies reported by the FINUDA collaboration in Refs. [1, 2], and the left side shows the theoretically calculated binding energies from Refs. [25, 26, 27, 28]. All the binding energies are measured from the  ${}^5\text{H} + \Lambda$  threshold.

the hyperon puzzle in this case. The baryon energy distribution in neutron stars predicts that a part of the baryons should be Lambda particles, but Lambdas can change most of temporary suggestions for EOS so that 1.4–1.5 of Solar masses should be limit, of a neutron star, while the mass of two of them is equal to 2 Solar masses [21]. Recently, the theory has suggested how to solve the problem [22] but new hypernuclear experimental data will help to choose the proper way.

First of all, the study of the  ${}^6_{\Lambda}\text{H}$  hypernucleus will be carried out with the  ${}^7\text{Li}$  beam:



We have chosen the  ${}^7\text{Li}$  beam because an extra proton from  ${}^7\text{Li}$  can be stripped by fragmentation, while an additional charge exchange reaction is necessary if a  ${}^6\text{Li}$  beam is used to produce the  ${}^6_{\Lambda}\text{H}$  hypernucleus. The probability of fragmentation is much higher than that of charge exchange reaction. Some discussion of the double charge exchange problem considering  ${}^6_{\Lambda}\text{H}$  hypernucleus production is presented, for example, by A.Sakaguchi [23].

An evidence from Frascati for three  ${}^6_{\Lambda}\text{H}$  hypernuclei has been reported [1, 2]. In the concluding remarks at the closing of the 11th International Conference on Hypernuclei and Strange Particle Physics (held in 2012 in Barcelona) the first observation of  ${}^6_{\Lambda}\text{H}$  was mentioned by T.Nagae [24] as one of the four main achievements in hypernuclear physics reached during the last years. On the other hand, the E10 collaboration in the J-PARC experiment did not observe a missing mass peak corresponding to the  ${}^6_{\Lambda}\text{H}$  production [4, 23]. However, A.Gal at the Barcelona Conference discussion noted that there will be low probability to see a signal from  ${}^6_{\Lambda}\text{H}$  in the J-PARC experiment due to the high transferred momentum and, consequently, the high momentum and excitation of the produced hypernuclei. Theoretical predictions are strongly model dependent

and controversial as well. For example, E.Hiyama and others have calculated [28] that  ${}^6_{\Lambda}\text{H}$  is not a stable nucleus and should decay into  ${}^4_{\Lambda}\text{H}+n+n$  if one takes into account the parameters of the  ${}^5\text{H}$  resonance measured up to now. At the same time there are estimates [29, 30] showing that the binding energy for  ${}^6_{\Lambda}\text{H}$  should be about a few MeV. So, it is necessary to carry out an experiment that can test  ${}^6_{\Lambda}\text{H}$  hypernucleus without doubt. At J-PARC, the search for  ${}^6_{\Lambda}\text{H}$  was continued as the phase-1 of the J-PARC E10 experiment which was performed at the J-PARC 50 GeV proton-synchrotron facility. However, the search for  ${}^6_{\Lambda}\text{H}$  by the  ${}^6\text{Li}(\pi^-, K^+)$  reaction at the pion beam momentum of 1.2 GeV/c gave no events again [23]. Considering the theory, it is necessary to cite A.Sakaguchi [23] at Sendai Conference:

“The results of the theoretical calculations indicate that the binding energy of  ${}^6_{\Lambda}\text{H}$  is sensitive to the interactions and the models employed in the calculations and also the structure of the  ${}^5\text{H}$  nucleus. The FINUDA collaboration also made another assignment of the 3 candidate events in which the 3 events of  ${}^6_{\Lambda}\text{H}$  corresponded to different states as shown in the most right part in Fig. 3 (we present this Figure from Sakaguchi’s paper as Fig. 4). The level structure of  ${}^6_{\Lambda}\text{H}$  still has ambiguities only with the FINUDA result, and complementary measurements are necessary (we emphasize this statement). The production mechanism by the DCX (double charge exchange) reaction and the structure of the neutron-rich  ${}^6_{\Lambda}\text{H}$  hypernuclei are not well understood, yet. More detailed analysis of the already obtained experimental data and further experimental studies of other neutron-rich  ${}^6_{\Lambda}\text{H}$  hypernuclei are necessary.”

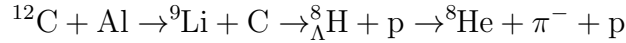
Anyway, it seems that if pion beams are used, the  ${}^6_{\Lambda}\text{H}$  production cross section is tiny, and more precise experiments with pion beams will be difficult. On the contrary, we suggest to use  ${}^7\text{Li}$  fragmentation due to much higher reaction probability instead of DCX of  ${}^6\text{Li}$ .

At this point one should note that in the Frascati and J-PARC experiments no hypernuclei were directly observed, only secondary effects like negative pions assumed as products of the  ${}^6_{\Lambda}\text{H}$  decay or the missing mass of a possible production reaction were determined. Since the statistics at Frascati were very low (3 candidates), and no signal was observed at J-PARC, the situation is controversial. Therefore, a crucial experiment can be carried out at the VBLHEP of JINR. The search for  ${}^6_{\Lambda}\text{H}$  with the HyperNIS spectrometer to obtain sufficiently high statistics (several hundred of detected events) should be done in order to measure the lifetime and production cross sections. This will provide a basis to solving the problem of whether hyperons indeed act as “glue” in the vicinity of the neutron rich drip line. Also, the mass of isotope the  ${}^6_{\Lambda}\text{H}$  can be measured using our magnetic spectrometer.

In fact, in the Dubna experiment, three isotopes of hydrogen hypernuclei ( ${}^3_{\Lambda}\text{H}$ ,  ${}^4_{\Lambda}\text{H}$ ,  ${}^6_{\Lambda}\text{H}$ ) should be produced simultaneously. It should be stressed that  ${}^3_{\Lambda}\text{H}$  and  ${}^4_{\Lambda}\text{H}$  can be used as a “reference points” to confirm the production and decay of  ${}^6_{\Lambda}\text{H}$ . Of course, the lifetimes of all these hypernuclear isotopes can be measured as well.

The production of hypernuclei with a large neutron excess and a neutron halo has been discussed by L.Majling since 1994 [31, 32]. The possibility of studying the baryon-baryon interaction in a system with an extremely large value of  $N/Z=6$  was pointed

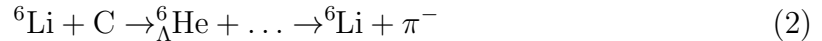
out. It was also emphasized that the measurement of  ${}^6_{\Lambda}\text{H}$  mass allows verification of the assumption that binding energy in neutron rich hypernuclei should be increased due to a specific “coherent  $\Lambda - \Sigma$  mixing mechanism” [33, 34]. It should be noted that there is a chain of four nuclei with two neutron halo and different composition of the  $S$ -shell core: with and without  $\Lambda$  hyperon, namely the nuclei  ${}^5\text{H}$ ,  ${}^6_{\Lambda}\text{H}$ ,  ${}^6\text{He}$ ,  ${}^7_{\Lambda}\text{He}$ . Thus, the study of the  ${}^6_{\Lambda}\text{H}$  properties (as well as of  ${}^6_{\Lambda}\text{He}$ ) will be significant for the theory. It was also noted that a  ${}^8_{\Lambda}\text{H}$  hypernucleus can be possible. If the first experiment with  ${}^6_{\Lambda}\text{H}$  is successful, the following search for the  ${}^8_{\Lambda}\text{H}$  hypernucleus will be the most natural aim. We propose to use  ${}^9\text{Li}$  beam for such an experiment. Also, it should be noted that the search for  ${}^8_{\Lambda}\text{H}$  using pion or kaon beams is even more difficult than the study of the  ${}^6_{\Lambda}\text{H}$ . The  ${}^9\text{Li}$  beam will be created as a secondary beam when carbon is accelerated. The chain of possible processes is as follows



The Lifetimes of  ${}^9\text{Li}$  and  ${}^8\text{He}$  are on the order of one hundred milliseconds, which is long enough for the experiment.

The expected production cross sections of the lightest hypernuclei are given in Table 1. New data from the present project will significantly improve the description of the hypernuclei production process. Taking into account these values, we have estimated possible counting rate for  ${}^4_{\Lambda}\text{H}$  pionic decays equal to 600 events per day in the case of ideal Nuclotron operation conditions (spill length of 5 s, no intensity pulsations, etc.). However, real tests have shown that this value should be reduced few times to 150-200 events per day because spill duration is shorter, we used lower beam intensity on the spectrometer because intensity pulsation causes overlapping of two beam particles inside 50 ns time interval with overlapping of signal amplitudes and so on. The properties of the Nuclotron extracted beam are continuously improving, but at this time the value of 150-200 events per day is the most realistic one. If we suppose that the binding energy of  ${}^6_{\Lambda}\text{H}$  is low, we can expect that its production cross section is of the same order as that of  ${}^3_{\Lambda}\text{H}$ . Then, one can expect to register 30-40 events of  ${}^6_{\Lambda}\text{H}$  per day. But we must admit that all estimates are based on the idea that coalescence is similar in all hydrogen hypernuclei production processes.

At the next stage of the experiment, **the  ${}^6_{\Lambda}\text{He}$  hypernuclei** will be investigated with the  ${}^6\text{Li}$  beam.  ${}^6_{\Lambda}\text{He}$  will be produced in peripheral Li interactions with a carbon target and the trigger will be tuned in order to select pionic decays with a negative pion and the daughter lithium nucleus emitted from the decay region:



It was established that the  ${}^6_{\Lambda}\text{He}$  hypernucleus is loosely bound (its neutron separation energy  $B = 0.17 \pm 0.10$  MeV). But its lifetime and production cross section were not measured up to now. **It is the  ${}^6_{\Lambda}\text{He}$  lifetime measurement which is the first task of the  ${}^6_{\Lambda}\text{He}$  experiment.** While  ${}^5_{\Lambda}\text{He}$  hypernuclei are investigated very well, it is not so easy to produce  ${}^6_{\Lambda}\text{He}$  hypernuclei in other experiments (that is why the study

Table 1: Measured and estimated hypernuclei production cross sections. Beam kinetic energy: GeV per nucleon; calculations are from ref. [8]. In  ${}^7\text{Li}$  beam on C target we have measured [35] the cross section of the charge change  $\sigma_{cc} = 650 \pm 20\text{mb}$ , this value is close to  $\sigma_{in}$ .

Beam	Hyper-nuclei	Energy (GeV)	Cross sec. ( $\mu\text{b}$ )	
			Theory	Exp.
${}^3\text{He}$	${}^3_{\Lambda}\text{H}$	5.14	0.03	$0.05^{+0.05}_{-0.02}$
${}^4\text{He}$	${}^3_{\Lambda}\text{H}$	3.7	0.06	$< 0.1$
	${}^4_{\Lambda}\text{H}$	2.2	0.08	$< 0.08$
		3.7	0.29	$0.4^{+0.4}_{-0.2}$
${}^6\text{Li}$	${}^3_{\Lambda}\text{H}$	3.7	0.09	$0.2^{+0.3}_{-0.15}$
	${}^4_{\Lambda}\text{H}$	3.7	0.2	$0.3^{+0.3}_{-0.15}$
${}^7\text{Li}$	${}^7_{\Lambda}\text{Li}$	3.0	0.11	$< 1$
	${}^6_{\Lambda}\text{He}$	3.0	0.25	$< 0.5$

of the  ${}^6_{\Lambda}\text{He}$  was stopped after emulsion experiments). Indeed, in kaon or pion beams  ${}^5_{\Lambda}\text{He}$  is produced if a  ${}^6\text{Li}$  target is used.

The method of the Coulomb dissociation suggested in refs. [17, 36, 37, 38] will be exploited for the **experimental estimation of the  ${}^3_{\Lambda}\text{H}$  and  ${}^6_{\Lambda}\text{He}$  binding energy**. This method is interesting from an experimental point of view since the interactions of hypernuclei “beam” should be investigated.

The Study of nonmesonic decays of the  ${}^{10}_{\Lambda}\text{Be}$  and  ${}^{10}_{\Lambda}\text{B}$  hypernuclei is planned in the present project as well. This study is aimed at the **determination of the  $\Lambda\text{N} \rightarrow \text{NN}$  weak interaction matrix elements** and implies measurements of the branching ratios  $\Gamma_{\alpha\alpha i}^{n(p)}$  for the exclusive decays of the  ${}^{10}_{\Lambda}\text{Be}$  and  ${}^{10}_{\Lambda}\text{B}$  hypernuclei [20, 39].

In such an experiment, one should register the chain of decays, for example,  ${}^{10}_{\Lambda}\text{B}$  which decays without the emission of a pion (nonmesonic decay) into  ${}^{10}_{\Lambda}\text{B} \rightarrow \text{n+p} + {}^8\text{Be}^*$  with subsequent  ${}^8\text{Be}^*$  decay emitting two  $\alpha$ 's within a very small angle. Since the two alpha particles and the decay products of the excited hypernuclei are emitted in a very narrow cone, the additional high resolution detectors should be installed to detect the twin alpha particles. Calculations have shown that GEM detectors of  $10 \times 10 \text{ cm}^2$  area can solve the problem. Additional trigger counter with thin (1 mm) quartz radiator can suppress the background by the factor of 30-50, coming from the beam nuclei fragmentation in the trigger detectors. Considering the spectrometer capability for such an experiment, we analyze and test the possibility to install several high resolution trackers, namely scintillating fiber detectors, GEM and microstrip detectors.



### 3 Spectrometer scheme

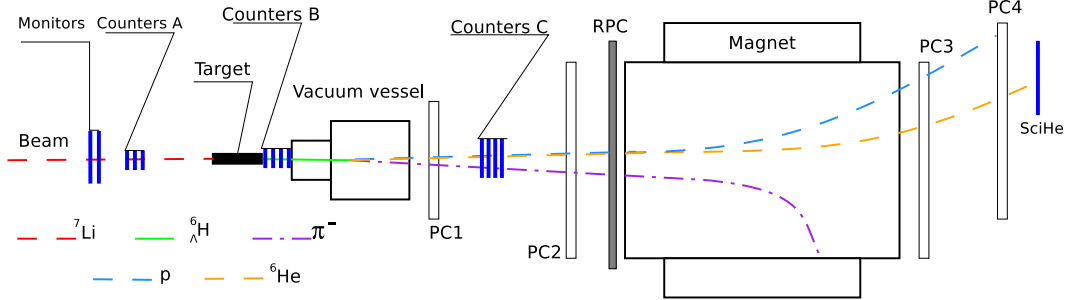
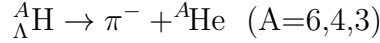


Figure 5: Configuration of the HyperNIS spectrometer. In particular for the search of  ${}^6_{\Lambda}\text{H}$  hypernuclei with the  ${}^7\text{Li}$  beam (not in scale). Target – carbon  $12 \times 3 \times 3$  cm,  $20.4 \text{ g/cm}^2$ ; beam monitors; A,B,C – trigger counters; vacuum decay vessel of 55 cm length; the analyzing magnet of 0.6T;  $PC_{1-4}$  – proportional chambers, RPC – TOF stations, SciHe – Scintillation counter to confirm registration of  ${}^6\text{He}$  nuclei.

Configuration of the spectrometer is presented in Fig. 5. In the  ${}^7\text{Li}$  beam nuclei interactions with carbon target ( $12 \text{ cm}$  along the beam and  $3 \times 3 \text{ cm}^2$  cross section,  $20.4 \text{ g/cm}^2$ ), when hypernuclei ( ${}^3_{\Lambda}\text{H}$ ,  ${}^4_{\Lambda}\text{H}$  or  ${}^6_{\Lambda}\text{H}$ ) are produced, pionic decay



will occur inside the vacuum vessel with rather high probability. The Čerenkov and scintillation counters (trigger detectors B,C correspondingly) are tuned to measure the charge difference between the hypernucleus and its decay products. Taking into account that the resolution of the Čerenkov counters is better, a block of four Čerenkov counters is used as B detector (as discussed above). Blocks of proportional chambers  $PC_1$  (four chambers  $38 \times 38 \text{ cm}^2$ ) and  $PC_2$  (two chambers  $130 \times 80 \text{ cm}^2$ ) register hits from the pion and the daughter nucleus (He), allowing the reconstruction of the decay vertex. In addition, the set of all proportional chambers ( $PC_{1-4}$ ) is used to measure the momentum of the He nucleus. The chambers  $PC_{3-4}$  are of the same size as the chambers  $PC_2$ . With the  ${}^7\text{Li}$  beam the full set of the chambers allows the detection of the secondary proton ( $p$ ) or another Li fragment and the momentum separation of the hydrogen hypernuclei daughter nuclei – He isotopes. The scintillation counter SciHe is used to measure and record the signal amplitude at the location where  ${}^6\text{He}$  daughter nuclei are expected to separate them between the tritium fragments produced together with  ${}^4_{\Lambda}\text{H}$  hypernuclei.

### 4 Experimental method

We underline four main features of the method elaborated at JINR. 1.) It is based on an idea to investigate high energy hypernucleus produced due to beam nucleus excitation. 2.) Such a hypernucleus decays outside the target that allows one to organize selective trigger and to identify produced isotopes separating the momenta of daughter nuclei. 3.) The trigger is tuned to find pionic decays of hypernuclei when the

charge of the daughter nucleus is higher than that of the hypernucleus and no physical event can simulate such a charge (and consequently counter signal) relation. 4.) Decay products are forward collimated, therefore the spectrometer acceptance is high. 5.) We analyze events when the hypernucleus decay vertex is observed in vacuum, where no background interaction can simulate the decay. 6.) Momenta of different hypernuclei isotopes are separated by large gaps (like momenta of daughter nuclei measured by the spectrometer), therefore it is easy to identify isotopes  ${}^3\text{He}$ ,  ${}^4\text{He}$  and  ${}^6\text{He}$ . In Fig. 6 we present the calculated  ${}^3\text{He}$ ,  ${}^4\text{He}$  and  ${}^6\text{He}$  momentum distribution for reactions

$${}^7\text{Li} + \text{C} \rightarrow {}^A_{\Lambda}\text{H} + p(d, t, n) + \dots \rightarrow {}^A\text{He} + \pi^- + p(d, t, n) \quad (A=6,4,3).$$

The following figure 7 shows that only in the case of large possible momentum mea-

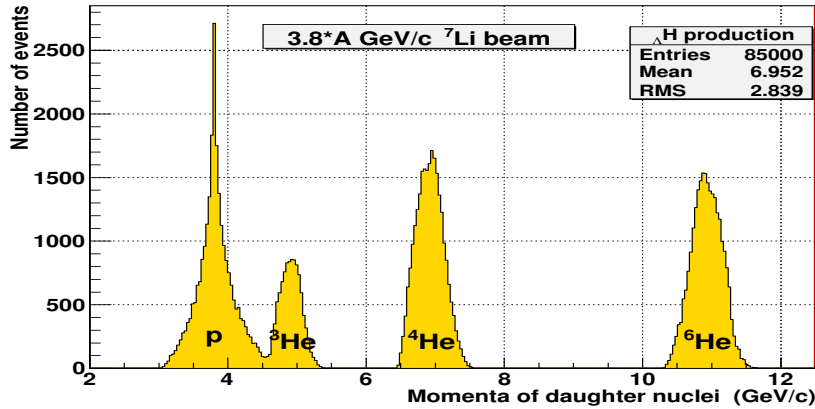


Figure 6: Expected distribution of He (hydrogen hypernuclei daughter nuclei) momenta values divided by their charge.  $P$  peak is the calculated momenta of protons produced in the Li fragmentation when  ${}^6_{\Lambda}\text{H}$  is produced. The peaks can be easily separated in order to identify different produced hyperhydrogen isotopes.

surment errors (for example  $-2\%$ ) peaks are clearly separated.

In order to measure the momenta of relatively slow pions, emitted at relatively large angles, the time-of-flight method will be used. For this purpose a wall of RPC chambers is installed in front of the analyzing magnet. The detector is effective for approximately 30% of the full pion spectrum and will be used to determine the mass of hypernucleus.

Also, it should be taken into account that the decay vertices can be found safely if the decay opening angle is not too narrow. We estimate that the efficiency of vertex reconstruction will be at a level of 90% because the opening angles are concentrated at higher values (see Fig. 11). In calculations presented above a minimal distance of 3 cm was chosen between He and pion hits in the proportional chambers to be sure that the decay vertex position can be reconstructed. However, this cut should be proved experimentally with high statistics of events when two particles leave a thin target. In 2021 two GEM detectors of  $40 \times 40$  cm in size will be obtained and installed in 2022 in order to reduce the number of events rejected due to a narrow opening angle (see below) and to increase the accuracy of hypernuclei decay point location. Thus,

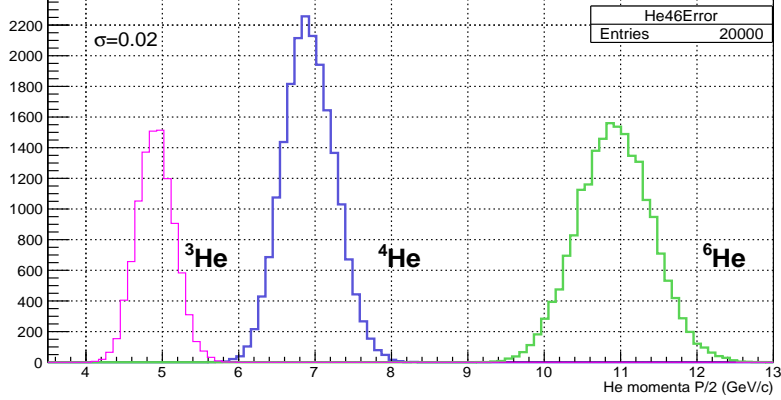


Figure 7: Expected distribution of He (hydrogen hypernuclei daughter nuclei) momenta values divided by their charge in case of 2% momenta error distribution. If  ${}^6_{\Lambda}\text{H}$  are produced  ${}^4_{\Lambda}\text{H}$  and  ${}^6_{\Lambda}\text{H}$  peaks can be easily separated.

tracking efficiency will be improved as well. All MC calculations have been done to choose the optimal geometry of target and proportional chambers. We should remind that the decay products, pions and daughter nuclei, are forward collimated so that we could find chamber positions to register more than 90% of decay pions. Of course, all daughter nuclei hit proportional chambers.

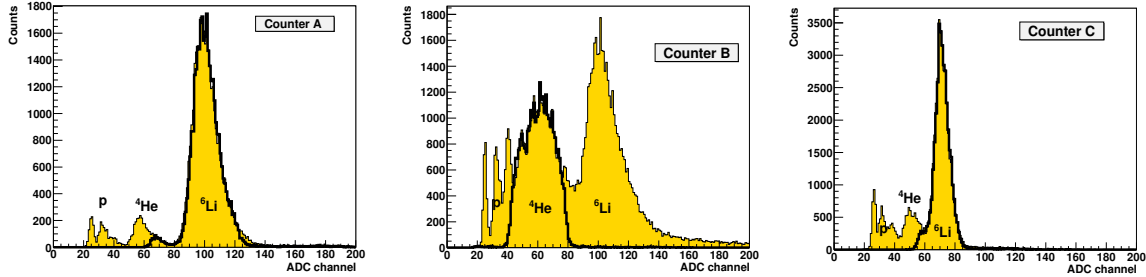


Figure 8: Tuning of trigger (scintillation) counters with  ${}^6\text{Li}$  beam for  ${}^6_{\Lambda}\text{He}$  production and decay. Example of signal amplitude spectra obtained for counters of beam monitors A, counters of sets B and C correspondingly. Signal amplitude peaks correspond to the lithium beam and its fragments from interactions with Al target inserted into the beam to produce different lithium fragments: helium, protons, deuterons. The thick line contours part of the spectrum determined by discriminators of counters A and C, which are tuned to register lithium, counter B – helium. As it was mentioned, scintillation counters B are replaced with Čerenkov counters now.

The trigger aimed to detect pionic decays of hypernuclei was developed and successfully used in the previous experiment in Dubna [5, 7, 20]. The idea of the trigger is as follows. When the  ${}^6_{\Lambda}\text{H}$  hypernucleus is produced, the Li nucleus should emit the spectator proton, while remaining core  ${}^6\text{He}$  nucleus is being changed into  ${}^6_{\Lambda}\text{H}$ . Each of these two particles have a charge equal to 1 (total  $Z = 1 + 1$ ) and hit block of the Čerenkov counters B. Since the counter response is proportional to  $Z^2$  of the interacting particle, both particles will create in the Čerenkov B counters the signals proportional to  $U = 1^2 + 1^2 = 2$ . Less than 2-3% (MC calculations) of associated  $K^+$  (slow, MC calculation) or recoil protons hit the Čerenkov counters B insensitive to slow particles.

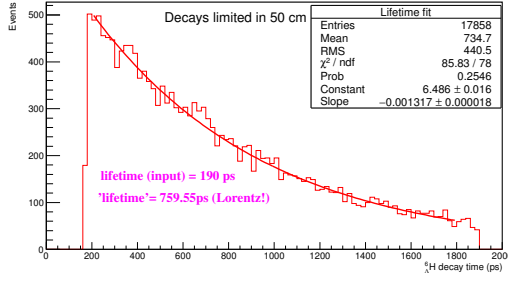


Figure 9: Expected decay time distribution inside of 50 cm distance. Due to the Lorentz factor the distribution is exponent with 760 ps decay parameter in case of 190 ps lifetime.

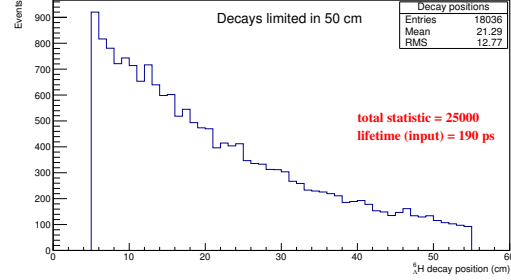


Figure 10: Expected decay points inside of 50 cm decay volume. 25000 events were analyzed and about 18000 hypernuclei decay inside of 50 cm distance which is 70% of the statistics if the first point is in 5 cm distance from the target.

Mesonic decay  ${}^6_{\Lambda}\text{H} \rightarrow {}^6\text{He} + \pi^-$  results into particles of  $Z = 2$  (He) and  $Z = 1$  ( $\pi^-$ ). The scintillation counters C of the minimal size are used in order to register only daughter nuclei. Most pions will miss these counters, and such a condition provides the best amplitude resolution of counters C. As for the spectator protons, it is expected that significant fraction of them will hit the counters. However, it is desirable to have a trigger working at full capacity, and therefore, one should ensure that the trigger works efficiently when the C counters have a signal proportional to  $U = 2^2 = 4$  (only He hits the C),  $U = 2^2 + 1^2 = 5$  (proton or pion also hits the counters), and  $U = 2^2 + 1^2 + 1^2 = 6$  (all the particles hit the C). Thus, in the counters C one should register a signal proportional to  $U \geq 4$  if the hydrogen hypernucleus decay takes place but less than  $U = 9$  created by the Li beam nuclei. Finally, we should underline that in the case of pionic decays the signal registered in the counters C is higher than that of B while for the majority of the background events the signal in C is lower than in B. Counters SciHe (see Fig 5) are not a part of the trigger, their signals are recorded and used to check that  ${}^6\text{He}$  was registered in chambers PC3, PC4 but not  ${}^3\text{H}$  background. Some results of the trigger tests were presented in [40, 41].

As noted above, a significant part of hypernuclei decays only after the target. For example, if one assumes the  ${}^6_{\Lambda}\text{H}$  hypernucleus lifetime to be equal to 190 ps than the  ${}^7\text{Li}$  beam of 27 GeV/c momentum (the highest value available at the beam line, 3.8 GeV/c per nucleon) produces hypernuclei with a lifetime at the laboratory frame of about 760 ps due to the Lorentz factor (see Fig. 9). It can provide a possibility to expect 70% of hypernuclei decays inside our vacuum vessel if it is located at a distance of 5 cm from the target (see Fig. 10).

In order to optimize the efficiency one should check if short distance between the target and the vacuumed decay volume does not cause additional losses due to the narrow angle between the pion and the hypernucleus daughter helium nucleus. Estimates show that a shorter distance between the target and the decay volume is a better choice. By increasing this distance, we lose statistics not only due to early decays, but also due to pions that miss the acceptance of the proportional chambers, while losses due to a narrow separation angle remain in 10-16 % interval and therefore are less significant. The distribution of the He-pion separation angle in the case of

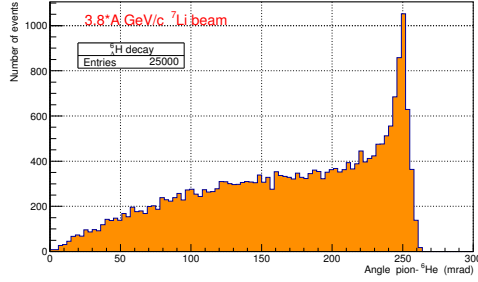


Figure 11: Distribution of the calculated pion helium separation angle in  ${}^6_{\Lambda}\text{H} \rightarrow \pi^- + {}^6\text{He}$  decays. About 10-16% decays of the have separation angles below the resolution of the proportional chambers but can be detected using GEM detectors in future experiments.

${}^6_{\Lambda}\text{H}$  decays is presented in Fig. 11, some results of the calculated pion distribution in proportional chambers are shown in Fig. 12,13.

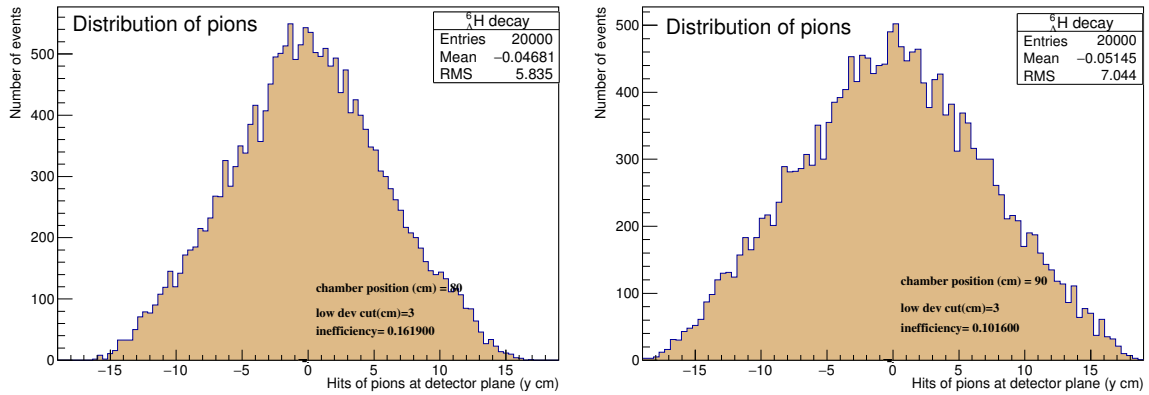


Figure 12: Distribution of pion hits in the proportional chamber situated at 80 cm (left) and 90 cm distance from the beam entrance point of the target. There are no decay pions outside the chamber. An arbitrary large cut of 3 cm distance between the He and pion hits is chosen as a limit of inefficiency, the cut in a real experiment will be optimized.

## 5 Last years results

During the Nuclotron run 50 the  ${}^7\text{Li}$  beam was for the first time delivered to the spectrometer. The obtained beam time was used mostly for tests and tuning of the modernized trigger system in the new counting room (located in a new place in the experimental hall). The background suppression factor which is much higher than  $10^4$  was reached.

Recently, a new tracking upgrade has been performed, the software has become more effective. Some results of tests using MC generated events are presented in Fig. 15,16.

In the last years the Nuclotron upgrade was the highest priority task for the laboratory. Therefore, it was necessary to wait until the extracted nuclear beam energy will

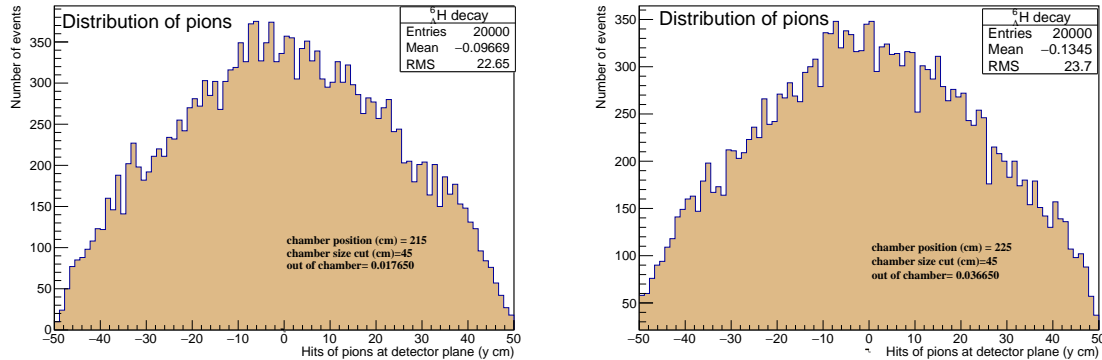


Figure 13: Pion hits at the last chamber to register pions. Geometric efficiency depends on a 10 cm shift of the target position in few percent loss. A distance of 215 cm is chosen for the experiment.

exceed the hypernuclei production threshold on such a value, which allows to carry out the hypernuclear experiments. Thus, the deuteron beam was used for short test runs in order to calibrate the spectrometer and to test new equipment. Data for proportional chambers alignment were taken, several alignment program codes were developed and investigated, all necessary calculations and fits were carried out. Some results are presented in Fig. 14.

Now the extracted nuclear beam kinetic energy has been increased up to 4 GeV/nucleon (well above the hypernuclei production threshold), the beam line to the HyperNIS spectrometer has been tested and the necessary nuclear beam has been transported to the spectrometer. Unfortunately, in 2017-2020, Li beam was available only for a short (63 hours) test run, which was used to tune the trigger for hypernuclei detection and to test chambers. This run was too short to start data taking.

On the other hand, the spectrometer has been significantly upgraded in recent years. Installation and testing of the time-of-flight detector [42] (RPC wall) in front of the analyzing magnet in order to determine the momentum of pions from decays of hypernuclei (by measuring the time of flight) was a serious step aimed to enhance the capability of the spectrometer. New electronic gas supply system (Fig. 17) allows one to stabilize and to improve time resolution. The results of the first tests are presented in Fig. 18. It should be mentioned that similar gas supply (Ethernet computer control possible) was installed for proportional chambers too.

But the most important improvement consisted of R&D and the production of new front-end electronics for proportional chambers. 200 analog signal cards (32 inputs in each card) were produced in Minsk. The digital part of the FEE cards (see Fig. 19,20) was designed and tested in JINR.

Electronic modules of the trigger system were replaced with new ones too. All modules in VME crate (TQDC modules, data acquisition and service modules as well) and the main DAQ server are new.

Systems of on-line service – beam control, monitoring of chamber efficiencies, slow control for high voltage supply units and others were elaborated, tested and used. Since

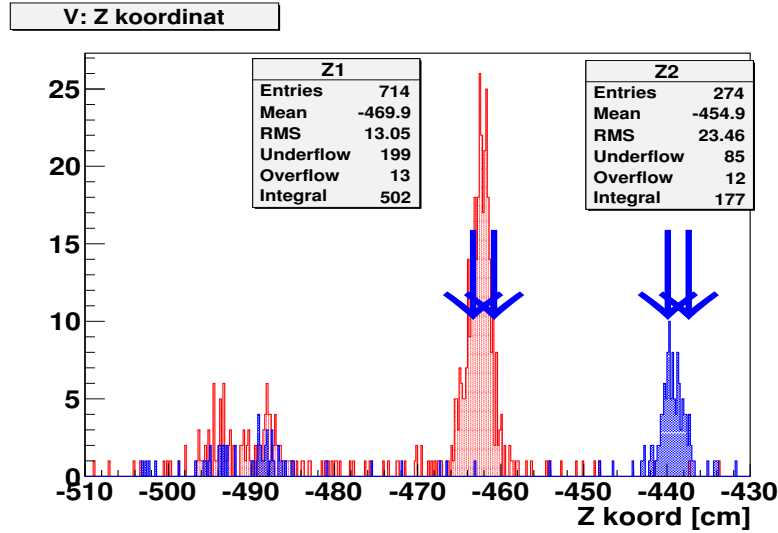


Figure 14: Position of the reconstructed  ${}^6_{\Lambda}\text{H}$  along the beam axis - results of testing alignment codes and vertex reconstruction procedure. The target was placed in two positions (red and blue histograms). The arrows show the edges of the target. The position of two monitor trigger counters can also be seen. The vertex position - the point of the minimal distance between the two tracks ( $d < 2\text{mm}$ ).

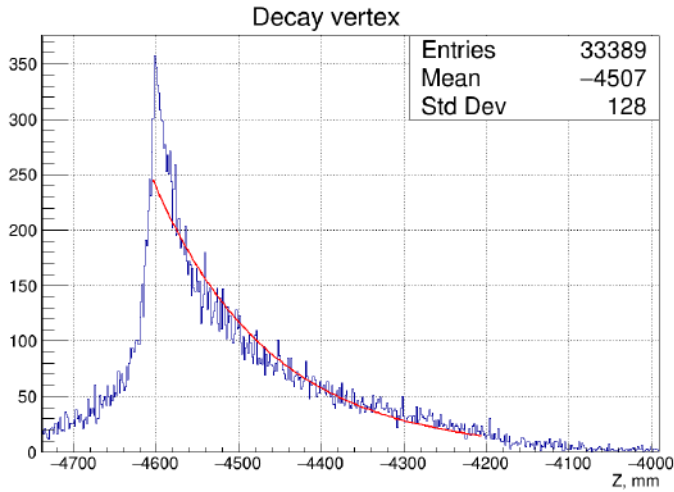


Figure 15: Properly reconstructed decay points allow one to measure the lifetime of the hypernucleus.  $Z = -4600\text{mm}$  is the beginning of the fiducial decay volume.

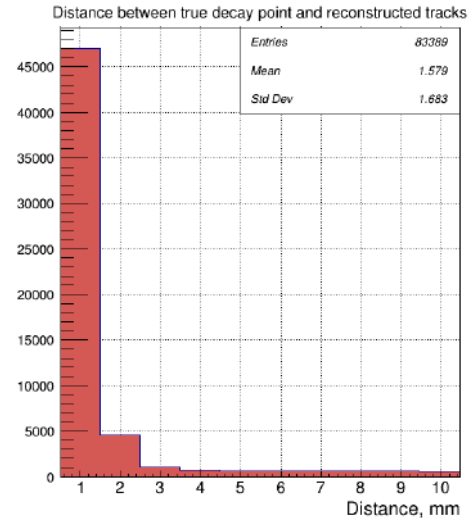


Figure 16: Decay points can be localized in two mm.

the beam intensity in the hypernuclei experiments is relatively low ( $10^5 - 10^6 \text{s}^{-1}$ ), it was necessary to organize Internet access to the beam control data for the Nuclotron staff. Moreover, taking into account the experience of test runs, this system is upgraded from run to run. All data from trigger counters are available in the Nuclotron control room and can be used by the staff to improve the beam tuning.

A new High Voltage supply system was introduced for trigger photomultiplier tubes. It has up to 64 high stability outputs driven by the WIENER MPOD crate controller and programs adapted by HyperNIS personal. Proportional chambers are driven using CAEN high voltage supply modules – see Fig. 21. In the time, low voltage systems for

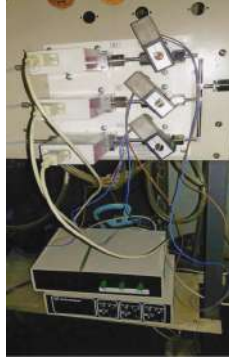


Figure 17: Electronic gas supply system of RPC.

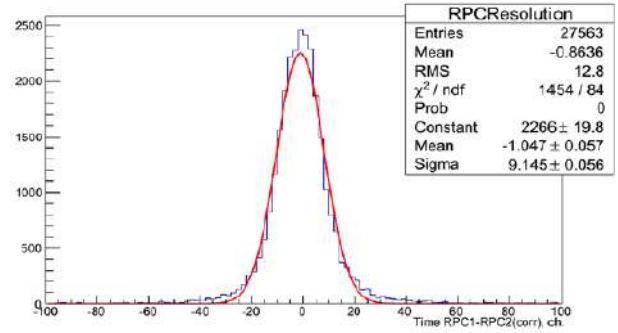


Figure 18: Time resolution of RPC chambers is equal to 180 ps.

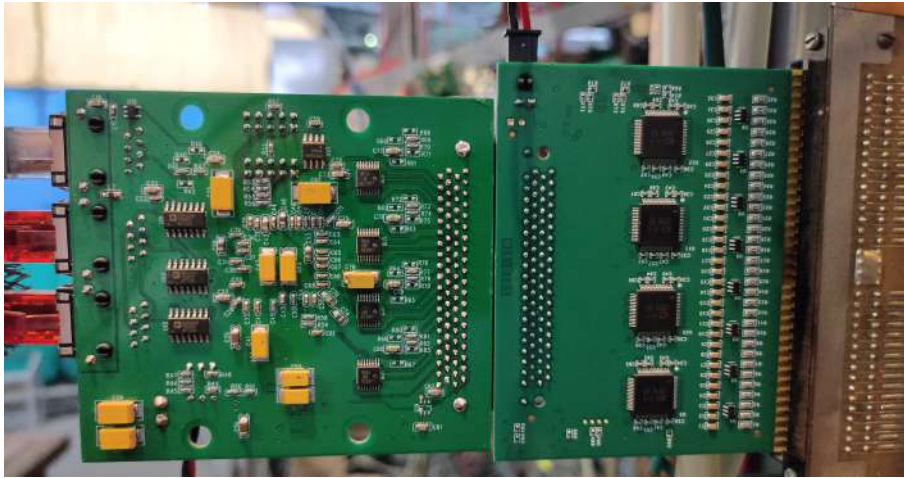


Figure 19: FEE cards: right – chamber output contacts and the analog signal amplifier part, left – the digital part for data processing and transfer.

proportional chambers were obtained and installed as well. Recently, a block of four Čerenkov trigger counters has been produced. the carbon target is located inside of the block close to the quartz radiators in order to minimize the losses of the observed hypernuclei due to decays (approximately 20% of the hypernuclei decay along the very first five centimeters after the target). The produced Čerenkov block was tested and the amplitude resolution higher than in the case of the scintillation counter block was obtained (see Fig. 22,23).

To reject the possible background of nuclear fragments produced in the trigger counters (primary tritium) several additional scintillation counters were produced and tested.

As a result, the spectrometer is prepared to carry out experiments dedicated to study neutron rich hypernuclei: the search for the hypernucleus  ${}^6_{\Lambda}\text{H}$  and the study of the properties, if it exists, the search for the  ${}^8_{\Lambda}\text{H}$  hypernucleus, the study of the hypernucleus  ${}^6_{\Lambda}\text{H}$ .

The most important technical result of the project is the commissioning of the multi-



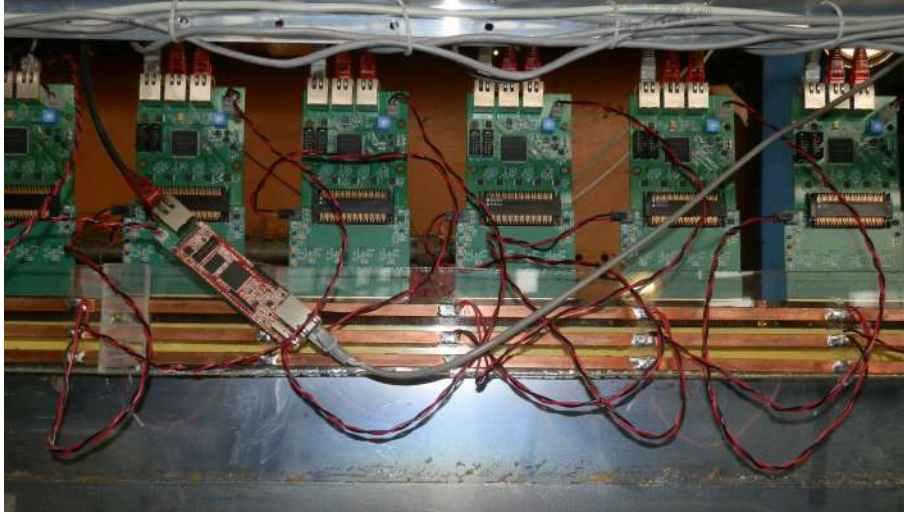


Figure 20: FEE cards on a proportional chamber.



Figure 21: NIM crate with CAEN high voltage power supply for proportional chambers.

purpose magnetic spectrometer with modern detectors and electronics which is ready for hypernuclear experiments using extracted Nuclotron beams. The spectrometer will also be available for other experiments (tests of detectors).

## 6 Present status of the apparatus.

After test runs on the Nuclotron beam, the HyperNIS spectrometer was commissioned. The extracted deuteron and  ${}^6\text{Li}$  as well as  ${}^7\text{Li}$  beams with kinetic energy of 1.0-3.5 GeV/nucleon and intensity of  $10^4 \div 10^5$  1/sec were used in the test runs of the Nuclotron.

To provide particles with different electric charges for the trigger tests, the  ${}^6\text{Li}$  beam passed through the Al target. The composition of the resulted beam after the target is

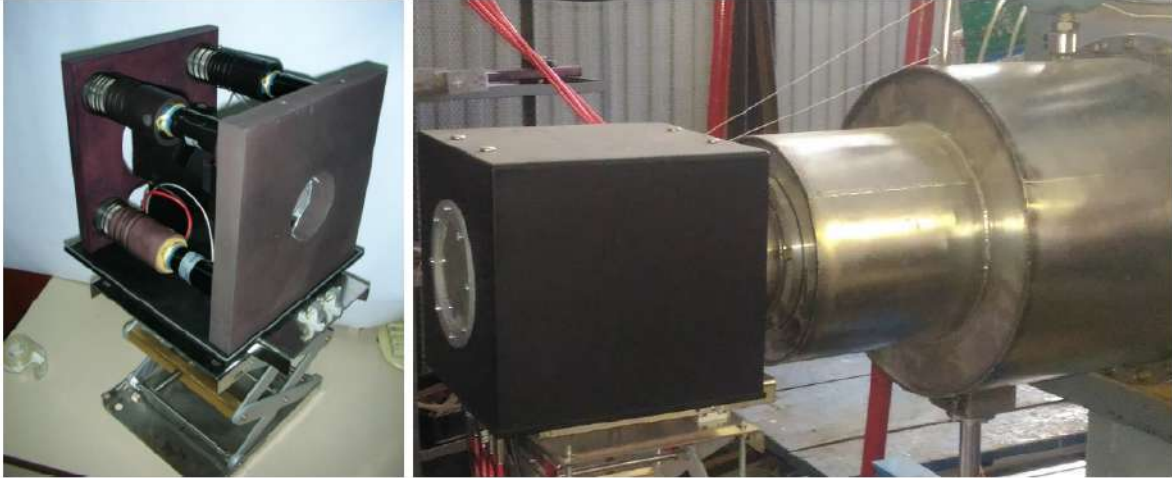


Figure 22: Block of 4 Čerenkov counters with 4 subsequent quartz radiators, 4 mm thick each. On the left side one can see 3 of 4 Electron Tubes 9107B photomultipliers. High density graphite ( $1.7 \text{ g/cm}^3$ ) target is placed close to radiators. The block itself is placed close to the vacuum vessel (right side of figure).

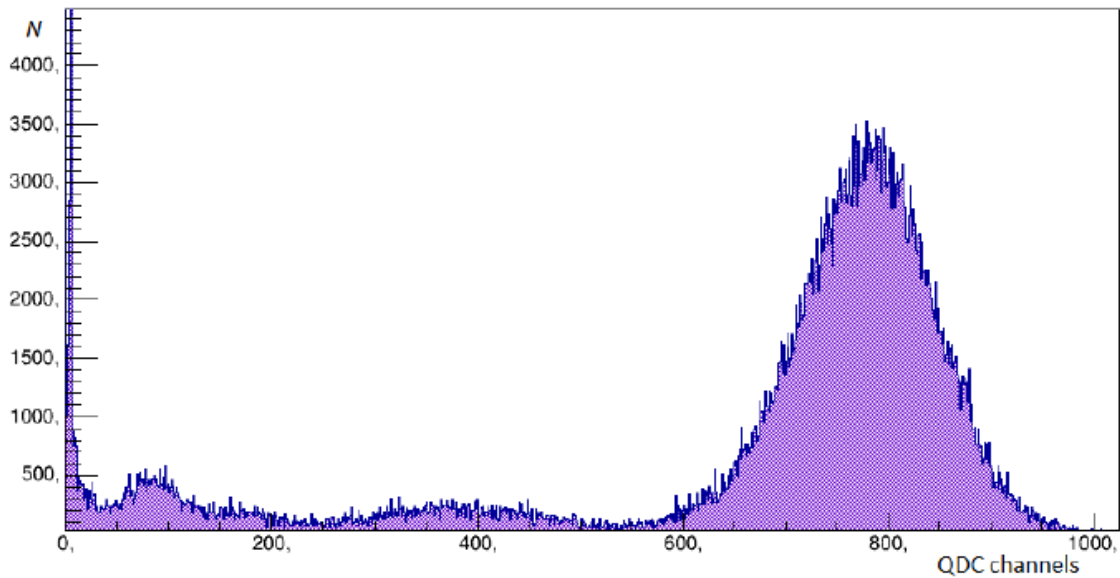


Figure 23: Pulse height distribution of Li beam fragments measured with one of the Čerenkov counters. Clean separation of p, He and Li particles is obtained.

shown in Fig. 8. Similarly, counters response linearity and resolution was tested with a carbon beam (see the example of the carbon and fragment signal amplitude spectrum in Fig. 24).

It should be noted once again that the trigger electronics has been upgraded in the last few years. Therefore, any possibility to have a beam was used to test the trigger for the hypernuclei study. Even if the beam was not suitable for hypernuclear experiments. While early tests give background suppression of the order of  $\sim 2.5 \cdot 10^3$  (see, for example [41]), background rejection of the order of  $\sim 10^4$  was achieved when a

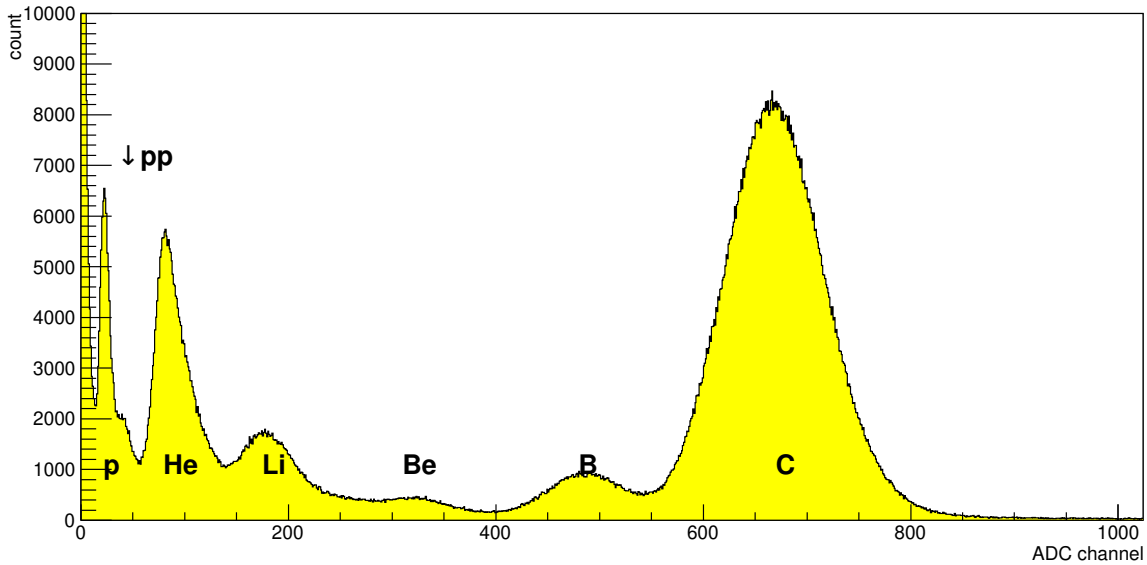


Figure 24: Amplitudes of a trigger scintillation counter measured with carbon beam and mixture of fragments (Al target in the beam).

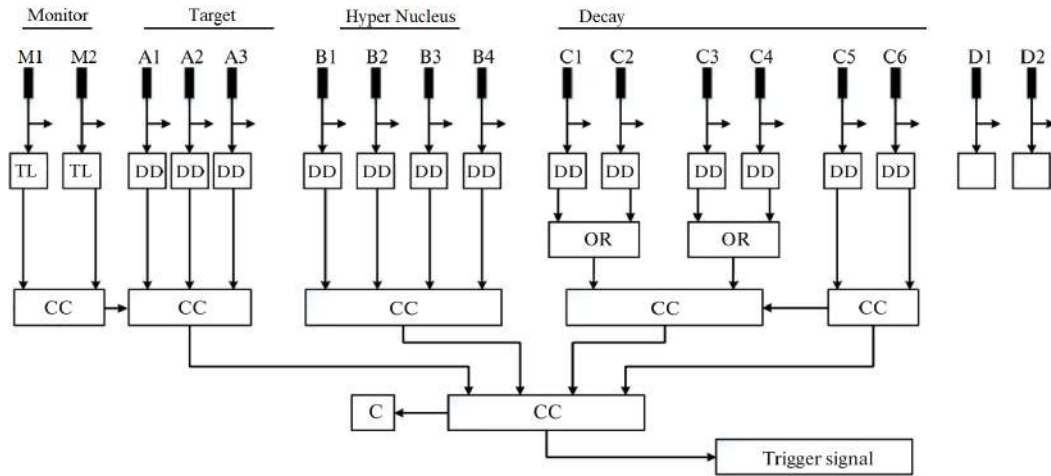


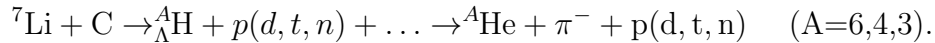
Figure 25: Trigger signal reception scheme: (filled rectangles) PEMS, (DD) differential discriminators, (TL) time locking scheme, (OR) logical adds, (CC) coincidence circuits, and (C) counting circuit.

test run with a  ${}^7\text{Li}$  beam was carried out. It should be added that we use two triggers simultaneously. One of them is aimed to search for the hypernuclei production and decay, while the second one is organized to check that the spectrometer performance is OK. Since the hypernuclei trigger rate is low, the second trigger was tuned to detect events every 100 msec when the MIP particle crosses the counters and proportional chambers. This trigger was used for checking the efficiency of all the chambers and for on-line control in the analysis of systematic errors.

The hypernuclei trigger must select events with the following signature: (i) “good”

incoming beam particles hitting the target are detected, i.e. particles with  $Z_{mon} = 3$ , for which no other particles appeared within the time interval  $\sim 30$  ns before and after it [43]. This selection is done by the “monitor” and “target” subsections of the trigger (Fig. 25) in coincidence; **(ii)** after the target, but before the decay region, a particle with a charge  $Z = Z_{mon} - 1$  was detected (the “hypernucleus” section in Fig. 25); **(iii)** after the decay region a particle with a charge  $Z = Z_{mon}$  was detected (the “decay” section in Fig. 25).

In case of detecting such a sequential change of the charge ( $3 \rightarrow (1 + 1) \rightarrow \geq 2 < 3$ ) the trigger generated a signal as shown in Fig. 25 for



A test run with the high energy ( $A \times 3.0$  GeV)  ${}^7\text{Li}$  beam and renovated trigger system located in the new counting room showed that the trigger can be tuned to suppress the background by a factor much higher than  $10^4$  [43]. As it was mentioned, 2 GEM detectors are on the way to JINR. The production of GEM detectors was postponed because the possible electronics was not ready. Now, the advance of GEM is readout electronics similar to that used in the LHEP experiments and it is possible to integrate it into our Data acquisition system (DAC). This detector improves the hypernuclei decay vertex search algorithm. If GEM is installed between trigger block B and the vacuum and registers three particles, we reject the event because all three particles are emitted from the target and do not originate from decay in the vacuum. Further, in 2021, the installation of two modern gas electron multipliers (CERN production) at the HyperNIS spectrometer is proposed. These detectors GEM1 and GEM2 will have the dimensions of an active area  $400 \times 400$  mm, 0.5mm between strips. We propose to install GEM1 in front of first block of proportional chambers and GEM2 behind it. Both of them will have space resolution near  $400 \mu\text{m}$  which allows to increase the angular accuracy for the track by factor of two. Furthermore, using these detectors will enlarge the useful statistics by 10% (nearly 15% events contain tracks within a narrow cone and can not be distinguished in the first MWPC now). Also, it improves the localization of the decay vertex point and, consequently, the accuracy of the lifetime measurements.

## 7 Conclusions

The study of the properties of the lightest hypernuclei is relevant, has high importance and can be performed in JINR with beams from the Nuclotron. The trigger of the HyperNIS spectrometer works with a high suppression factor and efficiency. The installation and commissioning of the new FEE allow us to significantly improve the tracking efficiency and to carry out the proposed hypernuclear experiments. This can give answers to open questions in hypernuclear physics which are very difficult to answer with alternative methods and approaches. As it was proposed, **the spectrometer is the best tool for the search and study of  ${}^6_{\Lambda}\text{H}$  and  ${}^8_{\Lambda}\text{H}$  neutron rich hypernuclei, it has a significant advantage if one investigates the  ${}^6_{\Lambda}\text{He}$**

**hypernucleus. As it was analyzed, the spectrometer is also aimed at the determination of the  $\Lambda N \rightarrow NN$  weak interaction matrix elements in the study of nonmesonic hypernuclei decays of  ${}^{10}_{\Lambda}\text{B}$  and  ${}^{10}_{\Lambda}\text{Be}$ .** To solve these tasks for a research program for 5-7 years we can start data taking in 2022.

Taking into account that the spectrometer site is suited for additional detectors, there is a possibility to install Short Range Correlations (SRC) experiment detectors so that detectors of both experiments are partly used for two tasks. The option is being analyzed to present a new project.

At present, the HyperNIS spectrometer is being tested using beta sources and cosmic muons. It should be noted that the HyperNIS spectrometer and the beam line can be easily used to test detectors. HyperNIS test runs were used (and can be used in future) to test pixel detectors (TimePix) from Prague (IEAP), microstrip detectors for satellite experiment, etc. TimePix tests were carried out together with the Prague team. These tests provided good experience for young Czech researchers. Also, several students for JINR were trained. Upgrade of the spectrometer, tuning of new modules and counters, test runs have shown that the HyperNIS team is ready to achieve the proposed aims.

## References

- [1] M.Agnelo et al., Phys.Rev.Lett. 108 (2012) 042501.
- [2] E.Botta, Nucl. Phys. **A914** 2013, 119.
- [3] M.Agnello et al., Nucl. Phys. **A881** 2012, 269.
- [4] H.Sugimura et al., J-PARC E10 Collaboration, Phys. Lett. B729 (2014) 39.
- [5] A.U.Abdurakhimov et al., Nuovo Cim. A102, (1989) 645.
- [6] S.A.Avramenko et al., Communication of JINR, Dubna, 1991.
- [7] S.Avramenko et al. Nucl. Phys. **A547** 1992, 95c.
- [8] H.Bandō et al., Nucl. Phys. A501, (1989) 900.
- [9] H.Bandō, T.Motoba and J.Žofka, Int. J. Mod. Phys. A5, (1990) 4021.
- [10] Y.Xu,... Proc. 12th Int. Conf. on Hypernuclear and Strange Particle Physics (HYP2015) JPS Conf. Proc. 17, 021005 (2017), <https://doi.org/10.7566/JPSCP.17.021005>.
- [11] S.Piano,...Proc. 12th Int. Conf. on Hypernuclear and Strange Particle Physics (HYP2015) JPS Conf. Proc. 17, 021004 (2017), <https://doi.org/10.7566/JPSCP.17.021004>.
- [12] C.Rappold, T.Saito, Proc. 12th Int. Conf. on Hypernuclear and Strange Particle Physics (HYP2015) JPS Conf. Proc. 17, 021003 (2017), <https://doi.org/10.7566/JPSCP.17.021003>.
- [13] H. Kamada, J. Golak, K. Miyagawa, H. Witala, W. Glöckle: Phys. Rev. C 57 (1998) 1595.
- [14] T. Motoba, et al.: Nucl. Phys. A 534 (1991) 597.
- [15] B. Donigus for the ALICE Collaboration, AIP Conference Proceedings 2130, 020017 (2019); <https://doi.org/10.1063/1.5118385>Published Online: 25 July 2019
- [16] L. Adamczyk et al. (STAR Collaboration) Phys. Rev. C 97, 054909 (2018)

- [17] S.A.Avramenko et al., Nucl.Phys. A585, (1995) 91c.
- [18] T.Saito, *Proceedings of the IX International Conference on Hypernuclear and Strange Particle Physics (HYP06), 2006, Mainz*, ed. by J.Pochodzalla and Th.Walcher (SIF and Springer-Verlag Berlin Heidelberg 2007) p.171.
- [19] C.Rappold et al., Nucl.Phys. A913 (2013) 170.
- [20] Yu.A.Batusov, J.Lukstins, L.Majling and A.N.Parfenov, Physics of Elementary Particles and Atomic Nuclei 36, (2005) 169.
- [21] Z. Azoumanian et al., Astrophys. J. Suppl. 235, (2018) 37, J. Antoniadis et al., Science 340, (2013) 1233232, H. T. Cromartie et al., Nature Astronomy 10.1038 (2019)
- [22] D.Logoteta, I.Vidana, and I.Bombaci, arXiv:1906.11722, Eur. Phys. J. A55 (2019) Article 207
- [23] Proc. 12th Int. Conf. on Hypernuclear and Strange Particle Physics (HYP2015) JPS Conf. Proc. 17, 011007 (2017), <https://doi.org/10.7566/JPSCP.17.011007>.
- [24] T.Nagae, Nucl. Phys. **A942** 2013, 559.
- [25] R.H. Dalitz and R. Levi Setti, Nuovo Cimento 30 (1963) 498.
- [26] Y. Akaishi and T. Yamazaki, Frascati Phys. Ser. XVI (1999) 59.
- [27] A. Gal and D.J. Millener, Phys. Lett. B725 (2013) 445.
- [28] E. Hiyama, S. Ohnishi, M. Kamimura and Y. Yamamoto, Nucl. Phys. A908 (2013) 29.
- [29] A.Gal, D.J.Millener, arXiv:1305.6716v4 [nucl-th] 28 Aug 2013.
- [30] B.F.Gibson, I.R.Afnan, Nucl. Phys. A (2014), in press.
- [31] L.Majling, Nucl. Phys. A585, (1995) 211c.
- [32] L.Majling, *Proceedings of the IX International Conference on Hypernuclear and Strange Particle Physics (HYP06), 2006, Mainz*, ed. by J.Pochodzalla and Th.Walcher (SIF and Springer-Verlag Berlin Heidelberg 2007) p.149.
- [33] K.S.Myint and Y.Akaishi, Progr. Theor. Phys. Suppl. 146, (2002) 599.
- [34] S.Shinmura et al., J. Physics G: Nucl. Part. Phys. 28, (2002) L1.
- [35] S.A.Avramenko et al., Communication of JINR P1-91-206, Dubna, 1991.
- [36] J.Lukstins, Nucl. Phys. A691, (2001) 491c.
- [37] S.V.Afanasiev et al., *Proceedings of the IX International Conference on Hypernuclear and Strange Particle Physics (HYP06), 2006, Mainz*, ed. by J.Pochodzalla and Th.Wacher (SIF and Springer-Verlag Berlin Heidelberg 2007) p.165.
- [38] M.V.Evlanov et al., Nucl. Phys. A632, (1998) 624; M.V.Evlanov et al., Particles and Nuclei, Letters 105, (2001) 5.
- [39] L.Majling and Yu.Batusov, Nucl. Phys. A691, (2001) 185c.
- [40] R.A.Salmin, O.V.Borodina, A.I.Maksimchuk, V.L.Rapatsky, talks at the LHE JINR Seminar on relativistic nuclear physics, June 06, 2007.
- [41] V.D.Aksinenko et al, *Proceedings of International Baldin seminar on high energy physics problems "Relativistic Nuclear Physics and Quantum Chromodynamics", Dubna, September 29 - October 4, 2008*), JINR, Dubna, 2008, p.155.
- [42] A. V. Averyanov, S. A. Avramenko, V. D. Aksinenko, A. N. Baeva, S. V. Gertsenberger, A. I. Golokhvastov, A. M. Korotkova, D. O. Krivenkov, J. Lukstins, A. I. Maksimchuk, E. A. Matyushina, O. V. Okhrimenko, N. G. Parfenova, S. N. Plyashkevich, R. A. Salmin, E. A. Strokovsky, and A. A. Feschenko, *Time-of-Flight System of HyperNIS Spectrometer*, ISSN 1547-4771, Physics of Particles and Nuclei Letters, 2019, Vol. 16, No. 6, pp. 796–806.

- [43] A. V. Averyanov, S. A. Avramenko, V. D. Aksinenko, A. N. Baeva, S. V. Gertsenberger, A. I. Golokhvastov, A. M. Korotkova, D. O. Krivenkov, J. Lukstins, A. I. Maksimchuk, E. A. Matyushina, O. V. Okhrimenko, N. G. Parfenova, S. N. Plyashkevich, R. A. Salmin, E. A. Strokovsky, and A. A. Feschenko, *Trigger System of the HyperNIS Experiment*, ISSN 1547-4771, Physics of Particles and Nuclei Letters, 2019, Vol. 16, No. 6, pp. 826–834.